Journal of
Nanoscience and Nanotechnology
Vol. 7, 1568–1572, 2007

A Comparative Study on SWCNT and DWCNT Field-Effect Transistors

X. L. Liang[1], S. Wang[1], X. J. Duan[2], Z. Y. Zhang[1], Q. Chen[1], J. Zhang[2], and L.-M. Peng[1,*]

[1] *Key Laboratory for the Physics and Chemistry of Nanodevices and Department of Electronics, Peking University, Beijing 100871, P. R. China*
[2] *Key Laboratory for the Physics and Chemistry of Nanodevices and College of Chemistry and Molecular Engineering, Peking University, Beijing 100871, P. R. China*

Field-effect transistors have been fabricated using single-walled carbon nanotubes (SWCNTs) and double-walled carbon nanotubes (DWCNTs), and their electrical transport properties have been studied comparatively. While a semiconducting SWCNT exhibits better field-effect characteristics than a DWCNT counterpart, the DWCNT shows more complicated response to external gate modulation. Depending on the nature of the two shells of a DWCNT, i.e., whether the shell is semiconducting (S) or metallic (M), a DWCNT device can be described as either S–S, or S–M, or M–S, or M–M. It was found that the S–S and M–M or M–S devices show similar field-effect characteristics to those found in SWCNT devices. But for S–M DWCNT devices, distinct field-effect characteristic was found and attributed to the combined effects of intershell interactions and screening by free carriers of the inner metallic shell. The S–M DWCNT devices thus provide a perfect system for studying the important intershell interaction, and information on the effect of this interaction on the electrical properties of a multi-walled carbon nanotube can be obtained by a comparative study of S–M DWCNT and S-SWCNT devices.

Keywords: SWCNT, DWCNT, FETs, Intershell Interaction.

1. INTRODUCTION

A carbon nanotube (CNT) can be considered as seamlessly folded graphene sheets, and according to the number of sheets involved a CNT may be classified either as single-walled CNT (SWCNT) or a multi-walled CNT (MWCNT). A SWCNT can be either metallic or semiconducting according to its folding helicity.[1] Due to its simple structure and unique electronic properties, SWCNTs were considered by many people to be the ideal building blocks for future nanoelectronics devices,[2,3] and received huge attention in recent years.[4–9] In comparison with SWCNTs, MWCNTs have several advantages, such as larger current carrying capacity.[10] Although the electrical transport of MWCNTs in high field has been investigated experimentally in last few years,[11–14] the intrinsic properties of MWCNTs still remain elusive because of their complicated structure and the lack of a clear understanding on the intershell interactions. For MWCNT devices, though usually the electrodes contact only the outmost shell of the tube directly, charges may be injected into inner shells via intershell interactions[12–14] and these injected charges in the inner shells are expected to affect the transport property of MWCNTs. To study the intershell interaction, the contribution to the total current by each individual shell should be separated because the current level in each shell reflects the strength of the interaction. However, experimentally it is still not possible to tell for sure as to how many shells are involved in the electric transport in a MWCNT, and to separate contributions from each shell since in general for a MWCNT both semiconducting (S)- and metallic (M)-shells are involved. In this regards double-walled carbon nanotubes (DWCNTs), being the simplest MWCNTs, are ideal systems for investigating intershell interactions, and a comparative study of SWCNTs and DWCNTs will be helpful in providing more information on the transport property and its dependence on the intershell interaction of MWCNTs. However, only a few experiments have been reported so far concerning with the electrical transport in DWCNTs.[15–17] In this work, field-effect transistors (FETs) have been fabricated using both SWCNTs and DWCNTs and their electrical transport characteristics have been investigated comparatively.

*Author to whom correspondence should be addressed.

 1533-4880/2007/7/1568/005 doi:10.1166/jnn.2007.340

2. EXPERIMENTAL DETAILS

The synthesis of SWCNTs and MWCNTs, which were used in this study, have been described in Refs. [18, 19]. The SWCNTs were directly grown on the silicon substrate while the DWCNTs were dispersed by sonication in dichlorethane and dropped onto Si substrate, in both cases the Si substrate was covered by a SiO_2 layer. The heavily doped Si substrate was used as a back gate and the thickness of the SiO_2 gate dielectric was 200 nm. After the positions of the CNTs were located using, e.g., atomic force microscope (AFM), Pd electrodes of 20 nm thick were defined by electron beam lithography. Transport properties of CNT FETs were measured using a Janis cryostat and a Keithley 4200 semiconductor characterization system.

3. RESULTS AND DISCUSSION

Figure 1(a) shows an AFM image of a typical SWCNT based FET, and Figures 1(b) and (c) show typical room temperature current–voltage (I–V) characteristics of a metallic SWCNT. The source–drain current (I_{ds}) changes linearly with the bias voltage (V_{ds}) and the current is basically independent of the gate voltage (V_g). Figure 2 shows similar results for a typical semiconducting SWCNT. The source–drain current varies non-linearly and saturates at large voltage. The I_{ds} is strongly gate voltage dependent and an ambipolar behavior is observed as the gate voltage sweeps. While the current in the "ON" state (with $V_g < -10$ V) is of the order of 10^{-6} A, the current at the "OFF" state (with $V_g \sim -7$ V to -2 V) is less than 10^{-11} A, and the on/off current ratio, I_{on}/I_{off}, was typically larger than 10^5 and 10^4 for the p- and n-region, respectively. The saturated current was completely depleted by the gate voltage in a range of about -5 V for p-region and -2 V for n-region, leading to an excellent field effect performance of the SWCNT based FET.

For a DWCNT (Fig. 3(a)), we may have four distinct shell–shell combinations, i.e., semiconducting (S)–S, metallic (M)–M, M–S, and S–M. Similar to a semiconducting SWCNT, where the current in the tube can be completely depleted, the current passing through a DWCNT can be completely depleted if both shells of the DWCNT are semiconducting, i.e., if the DWCNT is of the S–S type. On the other hand, when the transport of a CNT is dominated by current passing through a metallic channel the current can hardly be modulated by external gate due to strong screening of carriers in the metallic shell. For a DWCNT this condition may be satisfied if the DWCNT is either M–M or M–S, in both cases the conduction of the tube is dominated by the outer metallic shell.

Shown in Figure 3(b) is the room-temperature field effect characteristics of a S–S DWCNT. Typically for a S–S DWCNT based FET the I_{on}/I_{off} ratio is larger than 10^2, and depending on the diameter of the DWCNT it varies between 10^2 to 10^4. The current at the "OFF" state

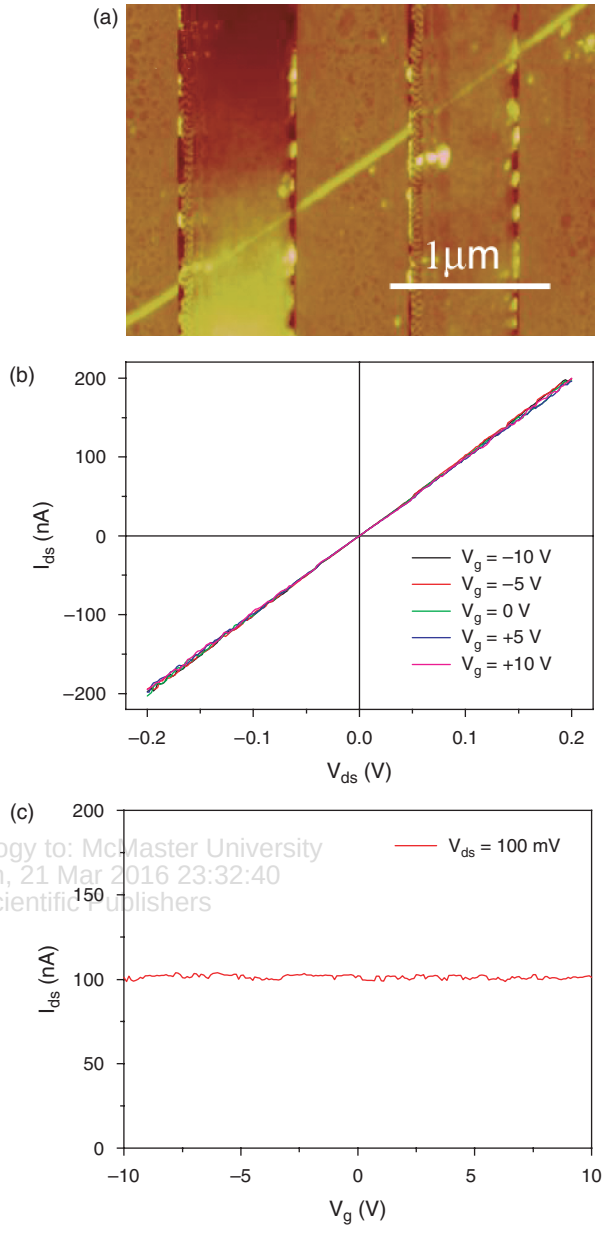

Fig. 1. (Color online) (a) An AFM image showing a typical SWCNT based FET. (b) I_{ds} versus V_{ds} and (c) I_{ds} versus V_g curves for a metallic SWCNT with a diameter of 1.8 nm and a length of 3 μm.

is usually larger than that associated with a SWCNT. This is because a DWCNT usually has a larger tube diameter and is more difficult to be depleted completely of carriers in both shells of the DWCNT. But typically the current level in the "OFF" state is less than 7×10^{-10} A. The current in the conducting DWCNT channels may thus be regarded to have been almost completely depleted. This response is very similar to the behavior of a semiconducting SWCNT as shown in Figure 2 and is consistent with our assumption that both shells of the DWCNT are semiconducting type. Figure 3(c) shows another type of I–V characteristics exhibited by a DWCNT based FET. The current is seen to hardly depend on the gate voltage

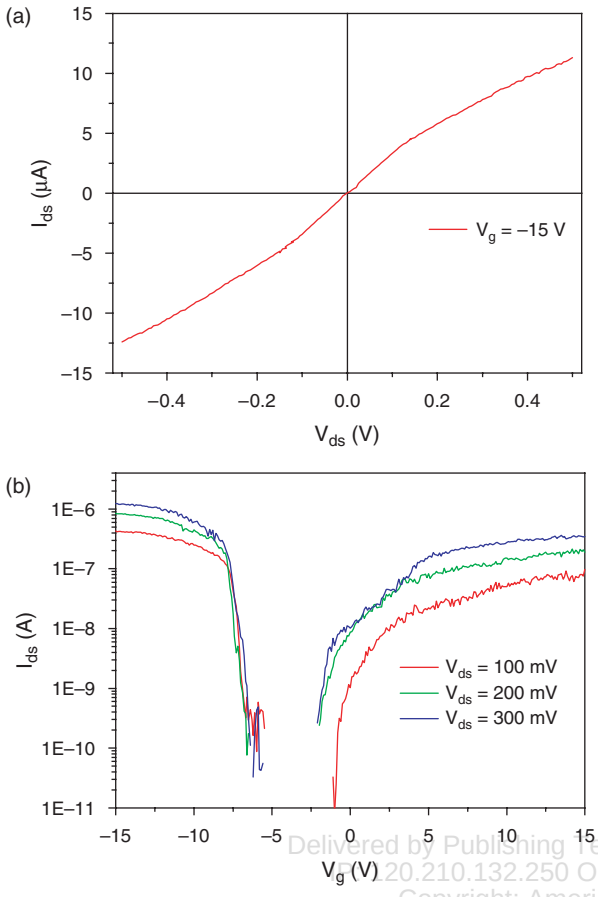

Fig. 2. (Color online) *I–V* characteristics of a semiconducting SWCNT. (a) I_{ds} versus V_{ds} and (b) I_{ds} versus V_g for a semiconducting SWCNT with a diameter of 2 nm and a length of 800 nm.

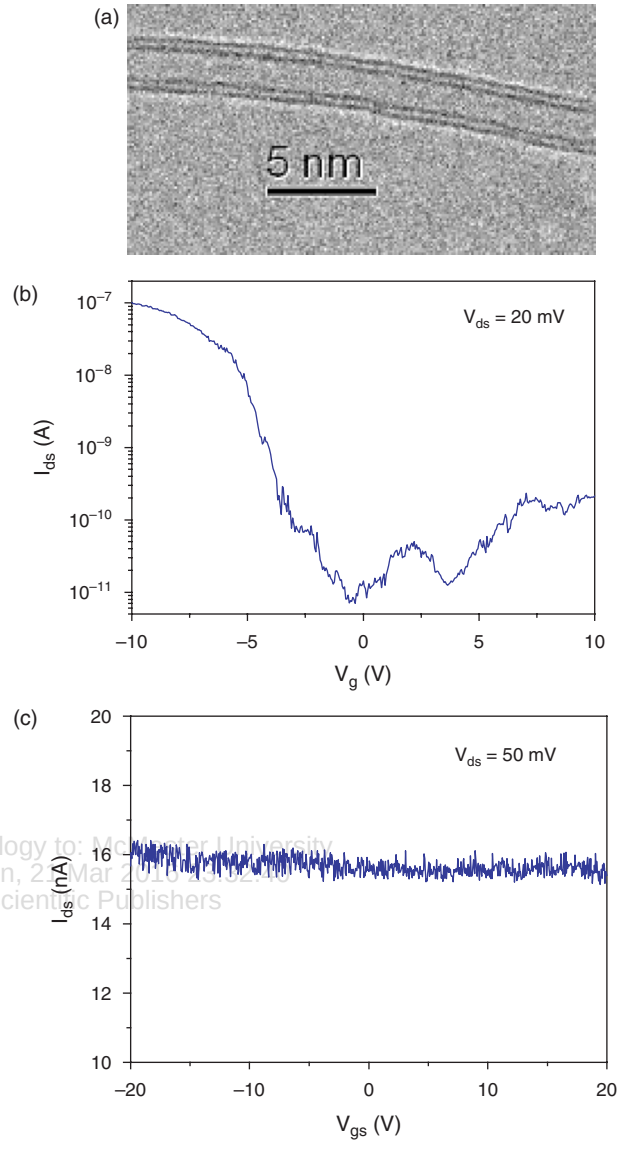

Fig. 3. (Color online) (a) TEM image showing a DWCNT. Typical room temperature I_{ds} versus V_g curves for (b) a S–S DWCNT with a diameter of 3 nm and a length of 600 nm and (c) a metallic DWCNT with a diameter of 4 nm and a length of 700 nm.

which is very similar to the typical response exhibited by a metallic SWCNT as shown in Figure 1(c). For this type of field-effect characteristics, however, we can not conclude uniquely as to whether a M–M or a M–S combination of shells is involved, since in both cases the conductance of the DWCNT is dominated by the outer metallic shell of the DWCNT. Therefore, the DWCNT involved in this behavior could be either M–M or M–S type.

While for a S–S DWCNT the conductance is dominated by semiconducting channel and a M–M or M–S DWCNT is dominated by metallic channel, the situation becomes much less clear when we are concerned with a S–M DWCNT. This type of DWCNTs shows distinct field-effect characteristics than that of the SWCNT, and a typical example is shown in Figure 4. In the *p*-region (with large negative gate voltage) both shells may contribute to the conductance. However, Figure 4 shows that for a S–M DWCNT the gate is much less effective in depleting carriers in the conducting channel. This is because finite number of carriers have been injected into the inner metallic shell of the S–M DWCNT, and it is these free carriers in the inner metallic shell that screen the outer S-shell from the effect of the gate and therefore prevent the DWCNT from complete depletion of carriers. In principle this effect provides a mean for investigating carrier distribution among the two shells of the DWCNT, and therefore the intershell interactions.

For a side-contacted S–M DWCNT device, the conductance is dominated by the outer S-shell when large negative gate voltage is applied (*p*-region). As the gate voltage is increased toward the *n*-region, the carrier density of the outer S-shell is decreased as the energy bands of this S-shell is lowered by the gate, and the finite carriers injected into the inner metallic shell begin to contribute to the conductance via intershell interactions and the residual current level in the *n*-region hardly changes once the outer S-shell is "turned off." This unique behavior, which

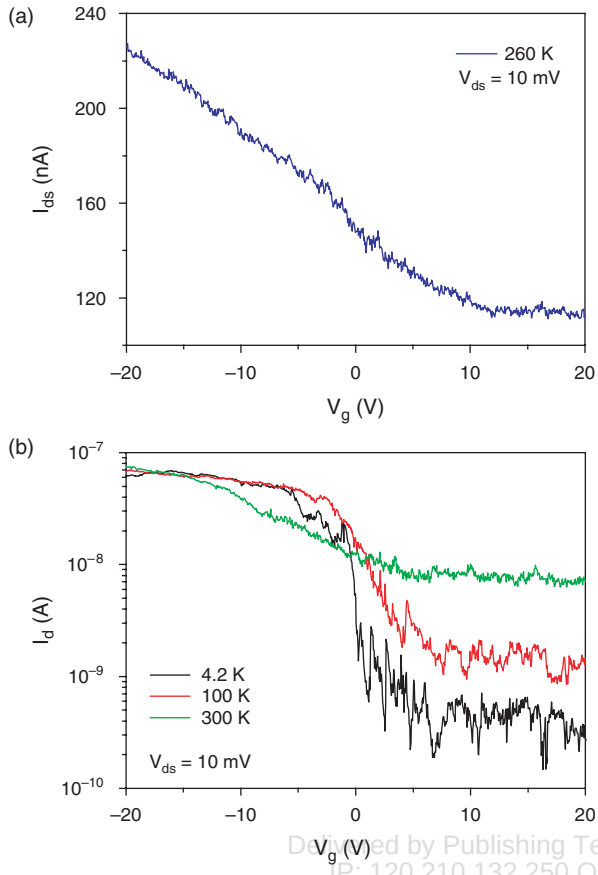

Fig. 4. (Color online) (a) Source-drain current versus gate voltage curve for a S–M DWCNT with a diameter of 4 nm and length of 400 nm. (b) Temperature dependence of I_{ds} versus V_g for a DWCNT with a diameter of 3 nm and a length of 400 nm.

stands for a S–M combination of the two shells, was confirmed by our latest controlled shell-by-shell breakdown experiments.[20]

Due to the strong intershell interaction the I_{on}/I_{off} ratio for a S–M DWCNT is typically less than 10, which is far lower than that can be achieved by S–S DWCNT FETs and SWCNT FETs of similar diameters. The transition region from the good hole-conduction (with $V_g < -10$ V) to the poor electron-conduction ($V_g > 10$ V) was found to be much wider than that found in both SWCNT and S–S DWCNT FETs. This is again due to the free charges in the inner metallic shell, since these free charges may rearrange themselves to reduce the effect of the gate on the DWCNT, i.e., charges in the inner metallic shell may screen the outer semiconducting shell from the influence of the gate to a certain extent. As a result, the *p*-type current associated with the S-shell was "turned off" much slowly and the *n*-type current cannot be "turned on" even for $V_g = 20$ V. The screening effect is strongly dependent on the available free charges in the inner metallic shell, and therefore electron injection efficiency or intershell interaction. Figure 4(b) shows that at lower temperature the current may be reduced to a very lower level, in agreement with previous work.[12, 14] As the temperature is lowered, fewer charges are injected into the inner metallic shell and screening effect is reduced. This results in narrower transition region and larger I_{on}/I_{off} ratio. Thus, the S–M DWCNT FETs behave like semiconducting SWCNT FETs at low enough temperature.

In an earlier work,[17] 200 DWCNT FETs were fabricated and 125 were found to function well. Among these 125 functioning devices 52 devices were found to show the typical S–S *I–V* field-effect response as shown in Figure 3(a), and this compares well with the simple geometric prediction that among 125 DWCNTs 55 should be S–S type; 44 devices were found to show hardly any change to gate voltage as shown in Figure 3(b) and this number is very close to the predicted number, i.e., 42; and the rest 29 devices show the S–M field-characteristics as shown in Figure 4, comparing with the predicted 28. Our classification of the field-effect characteristics of DWCNT FETs is further supported by controlled shell-by-shell breakdown experiments,[20] suggesting the important effect of the intershell interaction in the electron transport in MWCNTs.

In summary, SWCNTs and DWCNTs have been used to fabricate FETs and their transport properties have been studied. While for DWCNTs, the S–S, M–M or M–S, and S–M combination of the two shells have been distinguished according to their distinct field effect characteristics. A screening effect was found in S–M DWCNTs and comparative study of S–M DWCNTs and S-SWCNTs can obtain clear information of the intershell interaction of MWCNTs.

Acknowledgments: We thank Prof. H. M. Cheng for kindly providing the DWCNT samples used in this study. This work was supported by the Ministry of Science and Technology (Grant No. 001CB610502), National Science Foundation of China (Grant Nos. 10434010 and 60571002), and the Chinese Ministry of Education (Grant Nos. 10401 and 20030001071).

References and Notes

1. R. Saito, G. Dresselhaus, and M. Dresselhaus, Physical Properties of Carbon Nanotubes, Imperial College Press (**1998**).
2. C. Dekker, *Physics Today* 52, 22 (**1999**).
3. A. Bachtold, P. Hadley, T. Nakanishi, and C. Dekker, *Science* 294, 1317 (**2001**).
4. S. J. Tans, A. Verschueren, and C. Dekker, *Nature* 393, 49 (**1998**).
5. J. W. G. Wildoer, L. C. Venema, A. G. Rinzler, R. E. Smalley, and C. Dekker, *Nature* 391, 59 (**1998**).
6. T. W. Odom, J. L. Huang, P. Kim, and C. M. Lieber, *Nature* 391, 62 (**1998**).
7. S. J. Wind, J. Appenzeller, R. Martel, V. Derycke, and Ph. Avouris, *Appl. Phys. Lett.* 80, 3817 (**2002**).
8. M. Bockrath, D. H. Cobden, J. Lu, A. G. Rinzler, R. E. Smalley, L. Balents, and P. L. McEuen, *Nature* 397, 598 (**1999**).
9. A. Javey, J. Guo, Q. Wang, M. Lundstrom, and H. Dai, *Nature* 424, 654 (**2003**).

10. H. J. Li, W. G. Lu, J. J. Li, X. D. Bai, and C. Z. Gu, *Phys. Rev. Lett.* 95, 086601 **(2005)**.
11. S. Frank, P. Poncharal, Z. L. Wang, and W. A. de Heer, *Science* 280, 1744 **(1998)**.
12. P. G. Collins, M. S. Arnold, and P. Avouris, *Science* 292, 706 **(2001)**.
13. B. Bourlon, D. C. Glattli, B. Placais, J. M. Berroir, C. Miko, L. Forró, and A. Bachtold, *Phys. Rev. Lett.* 92, 026804 **(2004)**.
14. X. L. Liang, L. M. Peng, Q. Chen, R. C. Che, Y. Xia, Z. Q. Xue, and Q. D. Wu, *Phys. Rev. B* 68, 073403 **(2003)**.
15. M. Kociak, K. Suenaga, K. Hirahara, Y. Saito, T. Nakahira, and S. Iijima, *Phys. Rev. Lett.* 89, 155501 **(2002)**.
16. T. Shimada, T. Sugai, Y. Ohno, S. Kishimoto, T. Mizutani, H. Yoshida, T. Okazaki, and H. Shinohara, *Appl. Phys. Lett.* 84, 2412 **(2004)**.
17. S. Wang, X. L. Liang, Q. Chen, Z. Y. Zhang, and L. M. Peng, *J. Phys. Chem. B* 109, 17361 **(2005)**.
18. M. He, X. Duan, X. Wang, J. Zhang, Z. Liu, and C. Robinson, *J. Phys. Chem. B* 108, 12665 **(2004)**.
19. L. Li, F. Li, C. Liu, and H. M. Cheng, *Carbon* 43, 623 **(2005)**.
20. S. Wang, X. L. Liang, Q. Chen, K. Yao, and L. M. Peng, unpublished.

Received: 31 January 2006. Revised/Accepted: 7 June 2006.